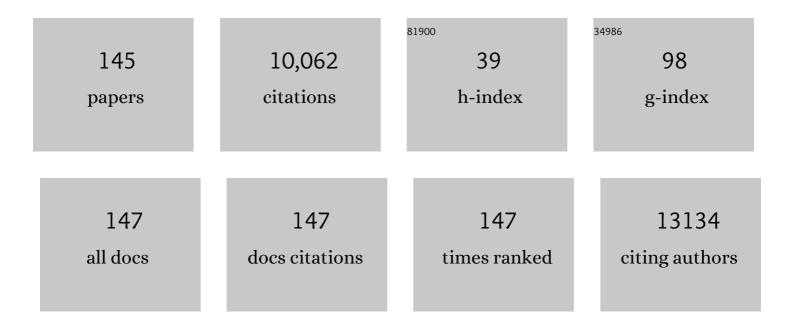
Hans-Gerd Boyen

List of Publications by Year in descending order

Source: https://exaly.com/author-pdf/7521493/publications.pdf Version: 2024-02-01



#	Article	IF	CITATIONS
1	The Role of SnF ₂ Additive on Interface Formation in All Leadâ€Free FASnI ₃ Perovskite Solar Cells. Advanced Functional Materials, 2022, 32, .	14.9	22
2	Operationally Stable Perovskite Light Emitting Diodes with High Radiance. Advanced Optical Materials, 2021, 9, 2100586.	7.3	13
3	Inkjet Printing of PEDOT:PSS Based Conductive Patterns for 3D Forming Applications. Polymers, 2020, 12, 2915.	4.5	28
4	Improved Field Electron Emission Properties of Phosphorus and Nitrogen Co-Doped Nanocrystalline Diamond Films. Nanomaterials, 2020, 10, 1024.	4.1	9
5	Lead-Halide Perovskites Meet Donor–Acceptor Charge-Transfer Complexes. Chemistry of Materials, 2019, 31, 6880-6888.	6.7	36
6	Laser-Patternable Graphene Field Emitters for Plasma Displays. Nanomaterials, 2019, 9, 1493.	4.1	5
7	Potentialâ€Induced Degradation and Recovery of Perovskite Solar Cells. Solar Rrl, 2019, 3, 1900226.	5.8	23
8	Fire Safety of Lead Halide Perovskite Photovoltaics. ACS Energy Letters, 2019, 4, 873-878.	17.4	42
9	Magnetic characterization of oblique angle deposited Co/CoO on gold nanoparticles. Journal of Magnetism and Magnetic Materials, 2019, 483, 76-82.	2.3	3
10	Environment versus sustainable energy: The case of lead halide perovskite-based solar cells. MRS Energy & Sustainability, 2018, 5, 1.	3.0	59
11	Electrocatalytic Behavior of Pd and Pt Nanoislands Deposited onto 4,4′-Dithiodipyridine SAMs on Au(111). Electrocatalysis, 2018, 9, 505-513.	3.0	10
12	Getting rid of anti-solvents: gas quenching for high performance perovskite solar cells. , 2018, , .		0
13	Compositional engineering of tin-lead halide perovskites for efficient and stable low band gap solar cells. , 2018, , .		7
14	Gas Quenching for Perovskite Thin Film Deposition. Joule, 2018, 2, 1205-1209.	24.0	67
15	Structure–Property Relations of Methylamine Vapor Treated Hybrid Perovskite CH ₃ NH ₃ Pbl ₃ Films and Solar Cells. ACS Applied Materials & Interfaces, 2017, 9, 8092-8099.	8.0	44
16	Reversible restructuring of supported Au nanoparticles during butadiene hydrogenation revealed by operando GISAXS/GIWAXS. Chemical Communications, 2017, 53, 5159-5162.	4.1	13
17	Synthesis and characterization of (Cd,Zn)S buffer layer for Cu2ZnSnSe4solar cells. Journal Physics D: Applied Physics, 2017, 50, 285501.	2.8	12
18	Band Gap Tuning via Lattice Contraction and Octahedral Tilting in Perovskite Materials for Photovoltaics, Journal of the American Chemical Society, 2017, 139, 11117-11124	13.7	570

#	Article	IF	CITATIONS
19	A Universal Deposition Protocol for Planar Heterojunction Solar Cells with High Efficiency Based on Hybrid Lead Halide Perovskite Families. Advanced Materials, 2016, 28, 10701-10709.	21.0	100
20	Assessing the toxicity of Pb- and Sn-based perovskite solar cells in model organism Danio rerio. Scientific Reports, 2016, 6, 18721.	3.3	396
21	Perovskite-perovskite tandem photovoltaics with optimized band gaps. Science, 2016, 354, 861-865.	12.6	1,107
22	Benchtop Fluorination of Fluorescent Nanodiamonds on a Preparative Scale: Toward Unusually Hydrophilic Bright Particles. Advanced Functional Materials, 2016, 26, 4134-4142.	14.9	36
23	Heat-transfer based characterization of DNA on synthetic sapphire chips. Sensors and Actuators B: Chemical, 2016, 230, 260-271.	7.8	10
24	Segregation Versus Colocalization: Orthogonally Functionalized Binary Micropatterned Substrates Regulate the Molecular Distribution in Focal Adhesions. Advanced Materials, 2015, 27, 3737-3747.	21.0	34
25	Improved nanodiamond seeding on chromium by surface plasma pretreatment. Chemical Physics Letters, 2015, 640, 50-54.	2.6	9
26	Organic phototransistors using poly(3-hexylthiophene) nanofibres. Nanotechnology, 2015, 26, 065201.	2.6	31
27	Nafion-Modified MoO _{<i>x</i>} as Effective Room-Temperature Hole Injection Layer for Stable, High-Performance Inverted Organic Solar Cells. ACS Applied Materials & Interfaces, 2015, 7, 3581-3589.	8.0	38
28	An electron beam evaporated TiO ₂ layer for high efficiency planar perovskite solar cells on flexible polyethylene terephthalate substrates. Journal of Materials Chemistry A, 2015, 3, 22824-22829.	10.3	116
29	The impact of precursor water content on solution-processed organometal halide perovskite films and solar cells. Journal of Materials Chemistry A, 2015, 3, 19123-19128.	10.3	55
30	Intrinsic Thermal Instability of Methylammonium Lead Trihalide Perovskite. Advanced Energy Materials, 2015, 5, 1500477.	19.5	1,788
31	Perovskiteâ€Based Hybrid Solar Cells Exceeding 10% Efficiency with High Reproducibility Using a Thin Film Sandwich Approach. Advanced Materials, 2014, 26, 2041-2046.	21.0	637
32	Detection of hydrogen peroxide vapor by use of manganese(IV) oxide as catalyst for calorimetric gas sensors. Physica Status Solidi (A) Applications and Materials Science, 2014, 211, 1372-1376.	1.8	21
33	Homopolymers as nanocarriers for the loading of block copolymer micelles with metal salts: a facile way to large-scale ordered arrays of transition-metal nanoparticles. Journal of Materials Chemistry C, 2014, 2, 701-707.	5.5	5
34	Ultrathin Ammonium Heptamolybdate Films as Efficient Room-Temperature Hole Transport Layers for Organic Solar Cells. ACS Applied Materials & Interfaces, 2014, 6, 16335-16343.	8.0	31
35	Relation between synthesis conditions, dopant position and charge carriers in aluminium-doped ZnO nanoparticles. RSC Advances, 2013, 3, 15254.	3.6	33
36	Ultrafast Selfâ€Assembly Using Ultrasound: A Facile Route to the Rapid Fabrication of Wellâ€Ordered Dense Arrays of Inorganic Nanostructures. Angewandte Chemie - International Edition, 2013, 52, 9709-9713.	13.8	7

#	Article	IF	CITATIONS
37	Hydrogen behaviour in amorphous Si/Ge nano-structures after annealing. Applied Surface Science, 2013, 267, 30-34.	6.1	9
38	Selective Protein Immobilization onto Gold Nanoparticles Deposited under Vacuum on a Protein-Repellent Self-Assembled Monolayer. Langmuir, 2013, 29, 15328-15335.	3.5	5
39	UV-induced functionalization of poly(divinylbenzene) nanoparticles <i>via</i> efficient [2 + 2]-photocycloadditions. Polymer Chemistry, 2013, 4, 4010-4016.	3.9	15
40	Impact of ammonium sulfide solution on electronic properties and ambient stability of germanium surfaces: towards Ge-based microelectronic devices. Journal of Materials Chemistry C, 2013, 1, 4105.	5.5	13
41	The use of XAFS to determine the nature of interaction of iron and molybdenum metal salts within PS-b-P2VP micelles. Physical Chemistry Chemical Physics, 2013, 15, 1675-1681.	2.8	3
42	Surface plasma pretreatment for enhanced diamond nucleation on AlN. Applied Physics Letters, 2013, 102, .	3.3	29
43	Controlled synthesis of ultrathin ZnO nanowires using micellar gold nanoparticles as catalyst templates. Nanoscale, 2013, 5, 7046.	5.6	15
44	A Molecular Toolkit for the Functionalization of Titaniumâ€Based Biomaterials That Selectively Control Integrinâ€Mediated Cell Adhesion. Chemistry - A European Journal, 2013, 19, 9218-9223.	3.3	53
45	Liquid-Phase Adsorption of Sulfur on Germanium: Reaction Mechanism and Atomic Geometry. Journal of Physical Chemistry C, 2013, 117, 7451-7458.	3.1	6
46	Interface-induced superconductivity in Pd films on SrS. , 2012, , .		0
47	Dewetting of Patterned Silicon Substrates Leading to a Selective Deposition of Micellar-Based Nanoparticles. Journal of Physical Chemistry C, 2012, 116, 10743-10752.	3.1	2
48	Hexagonal boron nitride nanowalls: physical vapour deposition, 2D/3D morphology and spectroscopic analysis. Journal Physics D: Applied Physics, 2012, 45, 135302.		
	analysis. Journal Physics D. Applieu Physics, 2012, 43, 133302.	2.8	22
49	Evidence for phase separation of ethanol-water mixtures at the hydrogen terminated nanocrystalline diamond surface. Journal of Chemical Physics, 2012, 137, 044702.	2.8 3.0	11
49 50	Evidence for phase separation of ethanol-water mixtures at the hydrogen terminated nanocrystalline		
	Evidence for phase separation of ethanol-water mixtures at the hydrogen terminated nanocrystalline diamond surface. Journal of Chemical Physics, 2012, 137, 044702.	3.0	11
50	Evidence for phase separation of ethanol-water mixtures at the hydrogen terminated nanocrystalline diamond surface. Journal of Chemical Physics, 2012, 137, 044702. Impact of Functional Groups onto the Electronic Structure of Metal Electrodes in Molecular Junctions. Journal of Physical Chemistry C, 2012, 116, 21810-21815. Generalized approach to the description of recombination kinetics in bulk heterojunction solar	3.0 3.1	11 8
50 51	 Evidence for phase separation of ethanol-water mixtures at the hydrogen terminated nanocrystalline diamond surface. Journal of Chemical Physics, 2012, 137, 044702. Impact of Functional Groups onto the Electronic Structure of Metal Electrodes in Molecular Junctions. Journal of Physical Chemistry C, 2012, 116, 21810-21815. Generalized approach to the description of recombination kinetics in bulk heterojunction solar cells— extending from fully organic to hybrid solar cells. Applied Physics Letters, 2012, 100, 203905. Magnetostructural effects in ligand stabilized Pd13 clusters: a density functional theory study. 	3.0 3.1 3.3	11 8 8

#	Article	IF	CITATIONS
55	Tracing Gold Nanoparticle Charge by Electrolyteâ^'Insulatorâ^'Semiconductor Devices. Journal of Physical Chemistry C, 2011, 115, 4439-4445.	3.1	16
56	Relationship between structural changes, hydrogen content and annealing in stacks of ultrathin Si/Ge amorphous layers. Nanoscale Research Letters, 2011, 6, 189.	5.7	10
57	Towards Efficient Hybrid Solar Cells Based on Fully Polymer Infiltrated ZnO Nanorod Arrays. Advanced Materials, 2011, 23, 2802-2805.	21.0	100
58	Hydrogen release in annealed hydrogenated aâ€6i/aâ€Ge multilayers. Crystal Research and Technology, 2011, 46, 877-880.	1.3	2
59	Superconducting state of very thin Pd films deposited on a diluted insulating EuxSr1â^'xS ferromagnet. Physical Review B, 2011, 83, .	3.2	4
60	Metallization of Ultraâ€Thin, Nonâ€Thiol SAMs with Flatâ€Lying Molecular Units: Pd on 1, 4â€Dicyanobenzene. ChemPhysChem, 2010, 11, 2951-2956.	2.1	14
61	A Molecular Double Decker: Extending the Limits of Current Metal–Molecule Hybrid Structures. Angewandte Chemie - International Edition, 2010, 49, 341-345.	13.8	28
62	Metallization of Organic Surfaces: Pd on Thiazole. Langmuir, 2010, 26, 4738-4742.	3.5	13
63	Chemical Interactions at Metal/Molecule Interfaces in Molecular Junctions—A Pathway Towards Molecular Recognition. Advanced Materials, 2009, 21, 320-324.	21.0	27
64	Mechanical and Tribological Properties of Epitaxial Cubic Boron Nitride Thin Films Grown on Diamond. Advanced Engineering Materials, 2008, 10, 482-487.	3.5	2
65	Purity of epitaxial cubic BoronNitride films on (001) Diamond — A prerequisite for their doping. Diamond and Related Materials, 2008, 17, 276-282.	3.9	19
66	Transition from anomalous kinetics toward Fickian diffusion for Si dissolution into amorphous Ge. Applied Physics Letters, 2008, 92, .	3.3	23
67	Magnetic moment of Fe in oxide-free FePt nanoparticles. Physical Review B, 2007, 76, .	3.2	41
68	Lowering of the L10 ordering temperature of FePt nanoparticles by He+ ion irradiation. Applied Physics Letters, 2007, 90, 062508.	3.3	66
69	Controlling the Interparticle Spacing of Auâ^'Salt Loaded Micelles and Au Nanoparticles on Flat Surfaces. Langmuir, 2007, 23, 10150-10155.	3.5	36
70	Fabrication of ohmic Au/Cr contacts on top of cubic Boron Nitride films. Diamond and Related Materials, 2007, 16, 46-49.	3.9	11
71	A Micellar Approach to Magnetic Ultrahigh-Density Data-Storage Media: Extending the Limits of Current Colloidal Methods. Advanced Materials, 2007, 19, 406-410.	21.0	103
72	Cavity ring-down spectroscopy of metallic gold nanoparticles. European Physical Journal D, 2007, 45, 501-506.	1.3	24

5

#	Article	IF	CITATIONS
73	Rhodium deposition onto a 4-mercaptopyridine SAM on Au(111). Electrochimica Acta, 2007, 52, 2740-2745.	5.2	40
74	From self-organized masks to nanotips: A new concept for the preparation of densely packed arrays of diamond field emitters. Diamond and Related Materials, 2006, 15, 1689-1694.	3.9	22
75	On the Morphology and Stability of Au Nanoparticles on TiO2(110) Prepared from Micelle-Stabilized Precursors. Langmuir, 2006, 22, 7873-7880.	3.5	27
76	Local density of states effects at the metal-molecule interfaces in a molecular device. Nature Materials, 2006, 5, 394-399.	27.5	98
77	Behaviour of discontinuous gold films on SrTiO3 substrates under annealing. Applied Surface Science, 2006, 253, 1160-1164.	6.1	5
78	Substrate influence in Young's modulus determination of thin films by indentation methods: Cubic boron nitride as an example. Surface and Coatings Technology, 2006, 201, 3577-3587.	4.8	39
79	Influence of ion induced amorphicity on the diffusion of gold into silicon. Journal of Applied Physics, 2006, 100, 063534.	2.5	6
80	Enhanced Orbital Magnetism inFe50Pt50Nanoparticles. Physical Review Letters, 2006, 97, 117201.	7.8	150
81	Electrical Resistivity of Epitaxial Au Films Surface-Modulated by Arrays of Pt Nanoparticles. European Journal of Inorganic Chemistry, 2005, 2005, 3691-3698.	2.0	3
82	From Colloidal Co/CoO Core/Shell Nanoparticles to Arrays of Metallic Nanomagnets: Surface Modification and Magnetic Properties. ChemPhysChem, 2005, 6, 2522-2526.	2.1	39
83	Electronic and Magnetic Properties of Ligand-Free FePt Nanoparticles. Advanced Materials, 2005, 17, 574-578.	21.0	67
84	Heteroepitaxial growth of cubic boron nitride films on single-crystalline (001) diamond substrates. Applied Physics A: Materials Science and Processing, 2005, 80, 735-738.	2.3	20
85	Metal deposition onto thiol-covered gold: Platinum on a 4-mercaptopyridine SAM. Surface Science, 2005, 590, 146-153.	1.9	87
86	Experimental evidence for a nonparabolic nanoscale interface shift during the dissolution of Ni into bulk Au(111). Physical Review B, 2005, 71, .	3.2	35
87	Effects of crystalline quality on the phase stability of cubic boron nitride thin films under medium-energy ion irradiation. Diamond and Related Materials, 2005, 14, 1482-1488.	3.9	16
88	Microstructure of the intermediate turbostratic boron nitride layer. Diamond and Related Materials, 2005, 14, 1474-1481.	3.9	34
89	Alloy Formation of Supported Gold Nanoparticles at Their Transition from Clusters to Solids: Does Size Matter?. Physical Review Letters, 2005, 94, 016804.	7.8	128
90	Resistivity and phonon softening in ion-irradiated epitaxial gold films. Journal of Applied Physics, 2004, 96, 7272-7277.	2.5	9

#	Article	IF	CITATIONS
91	Photon energy dependence of the dynamic final-state effect for metal clusters at surfaces. Physical Review B, 2004, 70, .	3.2	23
92	Properties of a Co/Cu/Co spin-valve system prepared by an optimized 193Ânm pulsed laser deposition process. Applied Physics A: Materials Science and Processing, 2004, 78, 327-333.	2.3	10
93	A New Approach to the Electrochemical Metallization of Organic Monolayers: Palladium Deposition onto a 4,4′-Dithiodipyridine Self-Assembled Monolayer. Advanced Materials, 2004, 16, 2024-2028.	21.0	115
94	Growth mechanism for epitaxial cubic boron nitride films on diamond substrates by ion beam assisted deposition. Diamond and Related Materials, 2004, 13, 1144-1148.	3.9	20
95	Effective exchange interaction in a quasi-two-dimensional self-assembled nanoparticle array. Physical Review B, 2004, 70, .	3.2	15
96	Growth of cubic boron nitride films on Si by ion beam assisted deposition at the high temperatures. Diamond and Related Materials, 2004, 13, 473-481.	3.9	22
97	Size effect of the resistivity of thin epitaxial gold films. Physical Review B, 2004, 70, .	3.2	116
98	Interface reactions in [Fe/B] n multilayers: a way to tune from crystalline/amorphous layer sequences to homogeneous amorphous Fe x B 100-x films. Applied Physics A: Materials Science and Processing, 2003, 76, 5-13.	2.3	8
99	A Micellar Route to Ordered Arrays of Magnetic Nanoparticles: From Size-Selected Pure Cobalt Dots to Cobalt–Cobalt Oxide Core–Shell Systems. Advanced Functional Materials, 2003, 13, 359-364.	14.9	113
100	Micellar Nanoreactors—Preparation and Characterization of Hexagonally Ordered Arrays of Metallic Nanodots. Advanced Functional Materials, 2003, 13, 853-861.	14.9	216
101	Epitaxy of cubic boron nitride on (001)-oriented diamond. Nature Materials, 2003, 2, 312-315.	27.5	133
102	Nanostructured surfaces from size-selected clusters. Nature Materials, 2003, 2, 443-448.	27.5	241
103	Depth profiles of Argon incorporated into Boron Nitride films during preparation and their temperature dependent evolution. Diamond and Related Materials, 2003, 12, 37-46.	3.9	15
104	The Self-organization of Metal Loaded Micelles - An Approach to Prepare Ordered Arrays of Metallic Nanoislands. Phase Transitions, 2003, 76, 307-313.	1.3	16
105	Characterization of ultrathin insulating Al2O3 films grown on Nb(110)/sapphire(0001) by tunneling spectroscopy and microscopy. Journal of Applied Physics, 2003, 94, 1478-1484.	2.5	19
106	Structural phase transitions in ZrO2 films induced by ion bombardment—Argon irradiation versus implantation. Journal of Applied Physics, 2003, 93, 5251-5254.	2.5	6
107	X-ray photoelectron spectroscopy study on gold nanoparticles supported on diamond. Physical Review B, 2002, 65, .	3.2	48
108	Influence of iron–silicon interaction on the growth of carbon nanotubes produced by chemical vapor deposition. Applied Physics Letters, 2002, 80, 2383-2385.	3.3	142

#	Article	IF	CITATIONS
109	Growth of thin, flat, epitaxial () oriented gold films on c-cut sapphire. Surface Science, 2002, 498, 168-174.	1.9	41
110	Oxidation-Resistant Gold-55 Clusters. Science, 2002, 297, 1533-1536.	12.6	484
111	Ion beam assisted growth of c-BN films on top of c-BN substrates — a HRTEM study. Diamond and Related Materials, 2002, 11, 38-42.	3.9	12
112	How to exploit ion-induced stress relaxation to grow thick c-BN films. Pure and Applied Chemistry, 2002, 74, 489-492.	1.9	3
113	Oxidation of preferentially (111)-oriented Au films in an oxygen plasma investigated by scanning tunneling microscopy and photoelectron spectroscopy. Surface Science, 2001, 475, 1-10.	1.9	128
114	Chemically Induced Metal-to-Insulator Transition inAu55Clusters: Effect of Stabilizing Ligands on the Electronic Properties of Nanoparticles. Physical Review Letters, 2001, 87, 276401.	7.8	62
115	Electronic structure of liquid tungsten studied by time-resolved photoelectron spectroscopy. Europhysics Letters, 2000, 49, 782-788.	2.0	13
116	Sequential ion-induced stress relaxation and growth: A way to prepare stress-relieved thick films of cubic boron nitride. Applied Physics Letters, 2000, 76, 709-711.	3.3	85
117	Fabrication of regularly arranged nanocolumns on diamond(100) using micellar masks. Journal of Applied Physics, 2000, 87, 7533-7538.	2.5	25
118	Time resolved valence band photoelectron spectroscopy of liquid palladium and molybdenum. Journal of Non-Crystalline Solids, 2000, 270, 1-5.	3.1	6
119	Ordered Deposition of Inorganic Clusters from Micellar Block Copolymer Films. Langmuir, 2000, 16, 407-415.	3.5	594
120	Thermoelectricity of disordered films near the metal–non-metal transition. Journal of Non-Crystalline Solids, 1999, 250-252, 791-794.	3.1	2
121	Electron spectroscopy on boron nitride thin films: Comparison of near-surface to bulk electronic properties. Physical Review B, 1999, 59, 5233-5241.	3.2	82
122	Electron energy loss spectroscopy—An additional tool to characterize thin films of cubic boron nitride. Diamond and Related Materials, 1998, 7, 385-390.	3.9	18
123	Intraband transitions in simple metals: Evidence for non-Drude-like near-IR optical properties. Physical Review B, 1997, 56, 6502-6505.	3.2	5
124	Angular momentum of conduction electron states. Journal of Non-Crystalline Solids, 1996, 205-207, 322-327.	3.1	1
125	Thermoelectric power and electrical resistance of thin, quench-condensed Sb/Au bilayers - a study of an amorphous phase at the interface. Journal of Physics Condensed Matter, 1996, 8, 6653-6663.	1.8	1
126	Photoelectron spectroscopy during pulsed laser melting of surfaces. Journal of Vacuum Science and Technology A: Vacuum, Surfaces and Films, 1996, 14, 2475-2479.	2.1	8

#	Article	IF	CITATIONS
127	Time-resolved valence band photoelectron spectroscopy of liquid AuSn. Journal of Physics Condensed Matter, 1996, 8, 9373-9377.	1.8	5
128	Photoelectron spectroscopic investigations of thin FexSi100â^'x films. Applied Surface Science, 1995, 91, 93-97.	6.1	18
129	Low-temperature interface reactions in layered Au/Sb films:In situinvestigation of the formation of an amorphous phase. Physical Review B, 1995, 51, 1791-1802.	3.2	18
130	Intermixing at Au-In interfaces as studied by photoelectron spectroscopy. Physical Review B, 1995, 51, 17096-17099.	3.2	10
131	Valence Band Photoelectron Spectroscopy of Liquid Silicon. Europhysics Letters, 1995, 31, 163-168.	2.0	16
132	Electronic structure ofNbxMo100â^'xsolid solutions. Physical Review B, 1995, 52, 16410-16414.	3.2	4
133	Surface core level shift for liquid and solid gallium. Journal of Non-Crystalline Solids, 1993, 156-158, 817-821.	3.1	1
134	Surface core level shifts in liquid metals and alloys. Journal of Non-Crystalline Solids, 1993, 156-158, 219-225.	3.1	2
135	Interplay of the atomic and electronic structure in liquid and amorphous Alî—,Ge alloys. Journal of Non-Crystalline Solids, 1993, 156-158, 236-240.	3.1	5
136	Core level binding energy shifts in liquid binary alloys: Auî—,Ga. Journal of Non-Crystalline Solids, 1993, 156-158, 241-245.	3.1	17
137	Electronic structure of amorphous Feî—,Zr alloys. Journal of Non-Crystalline Solids, 1993, 156-158, 246-250.	3.1	7
138	Synchrotron radiation study on amorphous Auî—,Sb and Auî—,Sn. Journal of Non-Crystalline Solids, 1993, 156-158, 259-262.	3.1	2
139	Core level shifts in amorphous transition metal-tin alloys. Journal of Non-Crystalline Solids, 1993, 156-158, 263-267.	3.1	1
140	Systematics in the electronic structure of amorphous transition metal/tin alloys. Materials Science & Engineering A: Structural Materials: Properties, Microstructure and Processing, 1991, 133, 107-110.	5.6	2
141	Electronic structure of disordered bismuth alloys: a comparison of the amorphous with the liquid state. Materials Science & Engineering A: Structural Materials: Properties, Microstructure and Processing, 1991, 133, 120-123.	5.6	2
142	Structure-Induced Minima in the Electronic Density of States—A Comparison of the Amorphous with the Liquid State. Europhysics Letters, 1991, 15, 759-764.	2.0	15
143	Influence of thermal relaxation and ion bombardment on the electronic properties of amorphous SiAu films. Journal of Physics Condensed Matter, 1990, 2, 7115-7122.	1.8	2
144	Photoemission valence-band structure of Hume-Rothery-type metallic glasses. Journal of Physics Condensed Matter, 1990, 2, 7699-7705.	1.8	11

#	Article	IF	CITATIONS
145	Comparison of amorphous and liquid alloys by photoelectron spectroscopy. Materials Science and Engineering, 1988, 99, 257-260.	0.1	18